Photoswitching of Salicylidene Methylamine: A Theoretical Photodynamics Study

Lasse Spörkel,[†] Joanna Jankowska,[‡,§] and Walter Thiel*,[†]

[†]Max-Planck-Institut für Kohlenforschung, Kaiser-Wilhelm-Platz 1, 45470 Mülheim an der Ruhr, Germany

[‡]College of Inter-Faculty Individual Studies in Mathematics and Natural Sciences, University of Warsaw, 93 Zwirki i Wigury St., 02-089 Warsaw, Poland

[§]Faculty of Chemistry, University of Warsaw, 1 Pasteura St., 02-093 Warsaw, Poland

Ⓢ Supporting Information

ABSTRACT: Photoswitching of simple photochromic molecules attracts substantial attention because of its possible role in future photon-driven molecular electronics. Here we model the full photoswitching cycle of a minimal photochromic Schiff base—salicylidene methylamine (SMA). We perform semiempirical nonadiabatic on-the-fly photodynamics simulations at the OM2/MRCI level and thoroughly analyze the structural time evolution and switching efficiency of the system. We also identify and examine in detail the crucial steps in the SMA photochemistry ruled by excited-state intramolecular proton transfer. The results place the investigated model aromatic Schiff base among the promising candidates for novel photoswitching molecular materials. Our study also shows the potential of the semiempirical multireference photodynamics simulations as a tool for early stage molecular photodevice design.
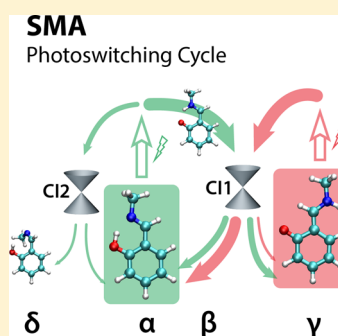
■ INTRODUCTION

Molecular photochromism and high photostability are among the crucial requirements for optically driven molecular memories, photoswitches, and data processing materials.[1−10] In this context special attention is paid to aromatic Schiff bases whose photochemistry is governed by an ultrafast excited-state intramolecular proton transfer (ESIPT).[11−18] In these molecules, the decay of the initially formed excited-state tautomer to the ground state can either lead back to the original species by proton transfer or trap a portion of the excited molecules in a ground-state metastable photochromic form. This opens prospects for applications in optically driven molecular devices.

Basic prerequisites for an efficient molecular photoswitch are the presence of at least two stable photochromic forms in the ground electronic state, lack of overlap between their absorption bands in the relevant excitation region, and radiationless decay routes from the Franck−Condon regions of both isomers leading to the other switching form. In the literature there are two main groups of chemical compounds investigated in the context of molecular photoswitching, which differ in their internal conversion mechanism: ring opening−ring closure versus cis−trans photoisomerization.[2,4,19] ESIPT-exhibiting aromatic Schiff bases introduce a novel way to optically driven switching control: here, the cis−trans photoisomerization is enabled (at least from one side) by the initial excitation of an enol-form allowing for a chemical bond rearrangement through proton transfer (PT).

In recent years the photophysics of aromatic Schiff bases has been intensively studied both experimentally and theoretically, and much progress has been made toward an understanding of the underlying mechanisms. However, in the context of molecular photoswitching, there are still important questions to be answered. In this paper we investigate the photochemistry and photoswitching properties of an isolated molecule containing the minimal Schiff base chromophore—salicylidene methylamine (SMA).

Despite its simple structure, SMA has been studied less than other model aromatic Schiff bases, such as salicylidene aniline (SA) or larger systems of similar type.[17,20−25] From the experimental side, the enol-form of SMA has been identified as the most populated ground-state isomer, and the photochromic behavior observed in solution has been attributed to the formation of the keto-form. The available experimental data (absorption and transient absorption spectra recorded in some nonprotic solvents[26,27]) indicate that no fluorescence signal is found upon UV−vis excitation in the absorption band of the enol-form of SMA. Moreover, only a very weak emission is observed for lower-energy excitation in the absorption band of the keto-form. This suggests that SMA undergoes a barrierless ESIPT process followed by efficient nonradiative internal conversion to the electronic ground state. Theoretical investigations of SMA photophysics performed so far include static energy landscape calculations and wave packet photodynamics simulations of the ESIPT process.[16,28,29] These studies confirm barrierless PT in the first singlet excited state
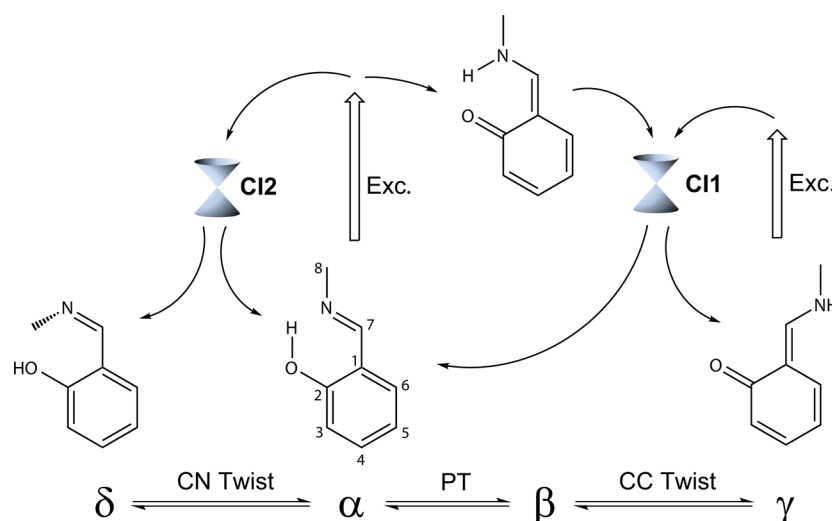
Figure 1. Chemical structures relevant for the photoswitching process and general scheme of the photochemistry of salicylidene methylamine.

Table 1. Relative Energies, Vertical Excitation Energies, and Important Geometrical Parameters for the Relevant Isomers and Conical Intersections of SMA Calculated with OM2/MRCI

	S_0 (kcal/mol)	S_1 (kcal/mol)	Vert. Exc. (eV)	OH (Å)	NH (Å)	$C_2C_1C_7N$ (deg)	$C_1C_7NC_8$ (deg)
α (S_0)	0.0	99.8	4.33	1.001	1.828	0.0	180.0
β (S_0)	5.6	75.3	3.02	1.649	1.047	0.0	180.0
γ (S_0)	11.4	87.1	3.28	4.674	1.013	180.0	180.0
δ (S_0)	6.8	112.6	4.59	0.995	2.693	60.3	0.4
α (S_1)	Relaxation to β (S_1)						
β (S_1)	13.3	68.0	2.37	1.696	1.039	0.0	180.0
γ (S_1)	22.0	76.4	2.36	4.604	1.018	180.0	180.0
δ (S_1)	Relaxation to CI2						
CI1	58.1	58.1	0.0	3.466	1.020	85.8	−153.7
CI2	60.2	60.2	0.0	0.997	1.961	5.4	90.9

of SMA and point to the presence of a conical intersection arising from CC double bond rotation as the main route for radiationless decay to the ground state.

In this work we present results of semiempirical on-the-fly photodynamics simulations for the two SMA tautomers relevant to photoswitching: the global minimum enol-form and the photochromic keto-form (denoted later as α and γ; for chemical structures see Figure 1). Our main goal is to investigate the full switching cycle and to determine the characteristic time scales and photoproduct distributions of both the forward and back switching transformations.

■ COMPUTATIONAL METHODS

The semiempirical calculations were performed using the OM2/MRCI method,[30−32] as implemented in the MNDO99 code.[33] During dynamics simulations, all required energies, gradients and nonadiabatic coupling elements were computed analytically.

The half-electron restricted open-shell Hartree−Fock (HF) formalism[34] was applied in the self-consistent field (SCF) treatment (i.e., the orbitals were optimized for the leading configuration of the S_1 state with two singly occupied orbitals). The active space in the multireference configuration interaction (MRCI) calculations included 10 electrons in 10 orbitals (see the Supporting Information for plots of these orbitals). In terms of the SCF configuration, it comprised the four highest doubly occupied orbitals, the two singly occupied orbitals, and the four lowest unoccupied orbitals. Three configuration state functions

were chosen as references for the MRCI treatment, namely the SCF configuration and the two closed-shell configurations derived therefrom (i.e., all singlet configurations that can be generated from the HOMO and LUMO of the closed-shell ground state). The MRCI wave function was built by allowing all single and double excitations from these three references. This semiempirical OM2/MRCI approach has been recently shown to perform well in a comprehensive general evaluation of excited-state properties[35] and in a number of recent excited-state studies.[25,36−48]

In trajectory surface-hopping dynamics the initial conditions are usually generated by Wigner sampling,[49,50] which defines initial coordinates and velocities based on classical or quantum harmonic vibrational modes, or by employing canonical classical molecular dynamics (MD) simulations, in which the canonical distribution is satisfied with the use of a thermostat. Here, we adopted the second approach applying the Nose-Hoover chains algorithm[51] (with a chain length of 10) for thermostatting. We used the default characteristic time of 0.01 ps for the thermostat and a time step of 1 fs for nuclear motion.

For both target molecules (α and γ isomers), ground-state MD runs were performed at the SCC-DFTB level.[52−54] 4 ps of equilibration dynamics were followed by a 100 ps production run, from which 600 initial atomic coordinates and velocities were randomly selected for each molecule. The starting points for the subsequent OM2/MRCI nonadiabatic dynamics were chosen from this set on the basis of the computed S_0 to S_1 transition probabilities and the vertical excitation energies. The
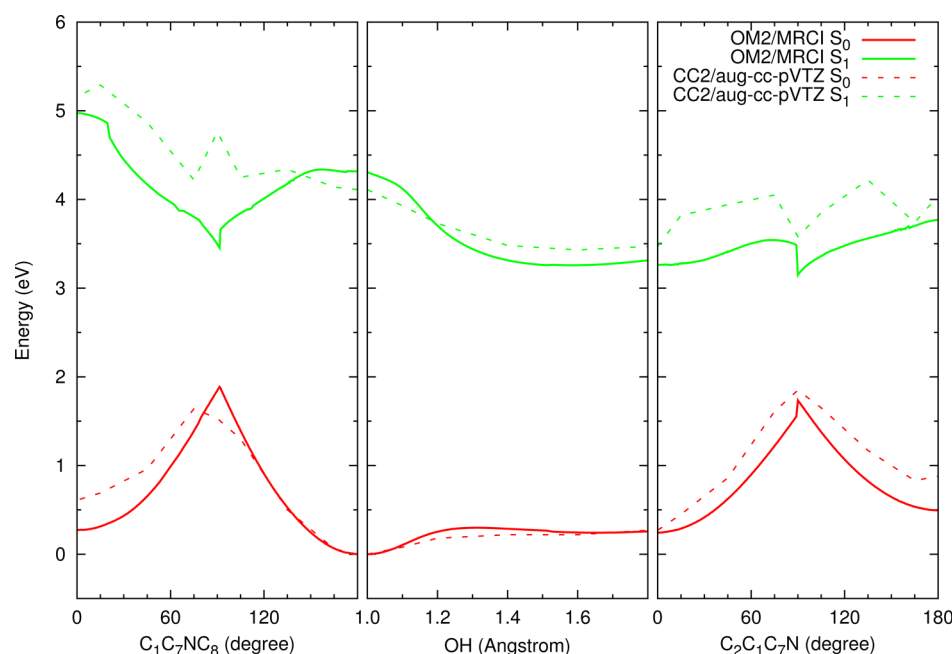
Figure 2. Vertical energy profiles for SMA calculated at the OM2/MRCI and CC2/aug-cc-pVTZ[29] levels (see text).

thermostat was switched off during the excited-state dynamics. A total of 321 surface-hopping trajectories for the α isomer and 333 for the γ isomer were run up to 1 ps with all relevant energies, gradients, and nonadiabatic coupling vectors being computed on-the-fly as needed.

For points with an $S_1 - S_0$ energy gap of less than 10 kcal/mol, the fewest-switches criterion was applied to decide whether to hop.[55,56] The time step was chosen to be 0.2 fs for nuclear motion and 0.0005 fs for electronic propagation. The unitary propagator evaluated at the middle point was used to propagate electronic motion.[57,58] Translational and rotational motions were removed in each step. The empirical decoherence correction (0.1 au) proposed by Granucci et al. was employed.[59] The final evaluations were done for the 259 α and 306 γ trajectories that finished successfully and satisfied our energy continuity criterion (no changes greater than 30 kcal/mol between any two consecutive MD steps). The SCC-DFTB sampling with the Nose-Hoover chains technique was done with ChemShell 3.4[60,61] and the nonadiabatic OM2/MRCI dynamics simulations were conducted with MNDO99.[33]

VALIDATION: STATIC CALCULATIONS

For specific validation of the OM2/MRCI method for SMA, the relevant isomers (see Figure 1) were optimized in the ground and first excited states. The two previously found S_1/S_0 conical intersections[29] were also located at the OM2/MRCI level. Table 1 lists the computed energies and selected geometrical parameters. The first excited state is always of $\pi\pi^*$ character in the OM2/MRCI calculations. For full geometrical structures and corresponding ab initio results see the Supporting Information (SI).

The OM2/MRCI results are consistent with the previously calculated energy landscape.[16,29] In the ground state the α conformer is confirmed to be the most stable form and all other isomers, except for δ, are found to be planar — as indicated by the given dihedral angles. In the first singlet excited state the α isomer does not correspond to a minimum but transfers the OH proton to the N atom upon geometry optimization,

forming the β isomer in a barrierless ESIPT process. In the course of the excited-state optimization the δ conformer relaxes to the CI2 conical intersection. The calculated vertical excitation energies to the S_1 state are reasonably close to the published values obtained from high-quality ab initio methods (CC2/aug-cc-pVTZ on MP2/cc-pVDZ geometries),[29] which are documented in the Supporting Information for easy reference.

For further validation, vertical potential energy profiles were calculated at the OM2/MRCI level and compared with corresponding ab initio data.[29] The profiles were computed for the variation of three geometrical parameters most relevant to SMA photochemistry: the $C_1C_7NC_8$ dihedral angle relating isomers α and δ (denoted as CN from now on), the OH distance relating isomers α and β, and the $C_2C_1C_7N$ dihedral angle relating isomers β and γ (denoted as CC from now on). For each point on the profile, the corresponding parameter was constrained to a fixed value and a full ground-state optimization was carried out for all other degrees of freedom. The energy of the first excited state was then obtained from a single-point calculation. The computed profiles are presented in Figure 2. The profiles obtained from the semiempirical OM2/MRCI calculations and from single-point ab initio CC2/aug-cc-pVTZ calculations on MP2/cc-pVDZ geometries are very similar to each other and agree with regard to all important features pertinent to SMA photochemistry. In particular, they show a barrierless proton transfer path in the first excited state and exhibit only very small barriers for the excited-state deactivation via CI1 and for the ground-state proton back transfer. The small bumps in the regions near the conical intersections are due to minor sudden changes in the optimized geometries.

DYNAMICS SIMULATIONS

Excited-state decay. After vertical excitation to the first singlet excited state, both the α enol-form and the γ keto-form of SMA undergo an ultrafast deactivation to the ground state. In both cases this process is usually finished after less than 300 fs. The average state populations during the α and γ
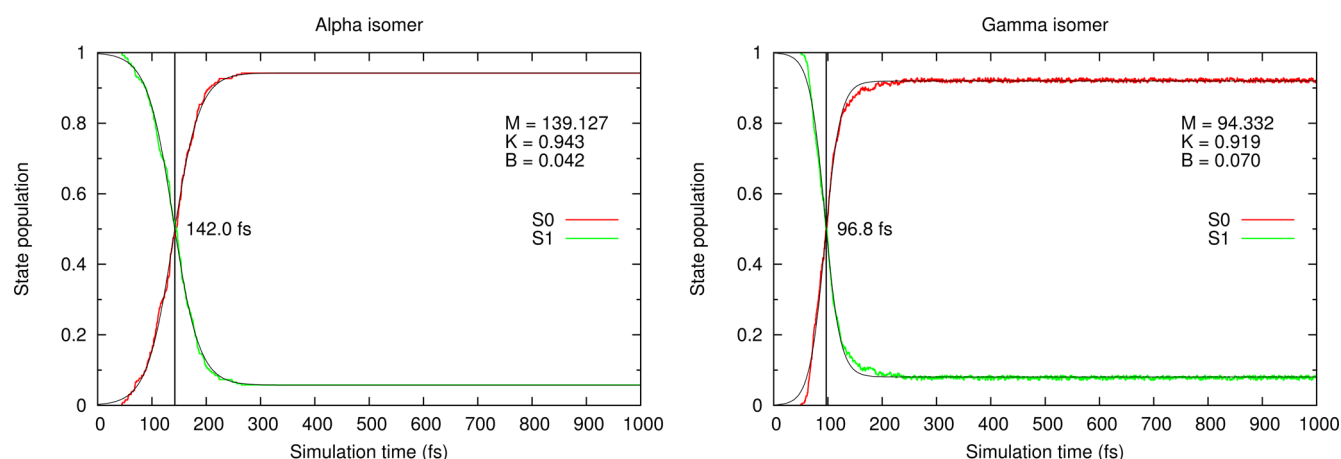
Figure 3. Average state populations for the two sets of trajectories (left: α isomer; right: γ isomer). The parameters of the sigmoidal fitting function are specified in the plots.
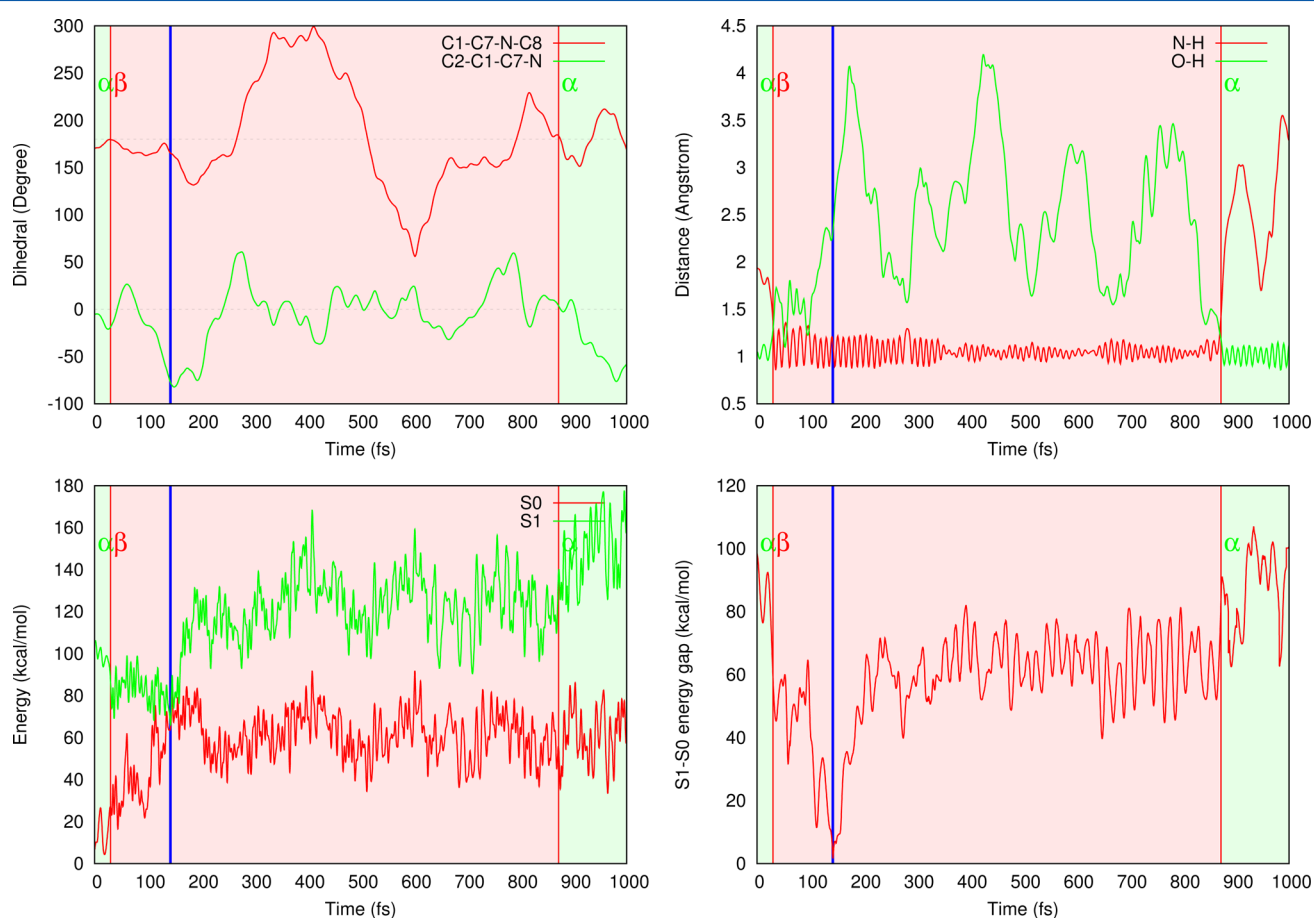

Figure 4. Different properties vs simulation time of a typical trajectory for the α isomer. Top left: dihedrals, horizontal dashed lines mark multiples of 180°; top right: distances; bottom left: state energies; bottom right: energy difference.

photodynamics are plotted in Figure 3 against the simulation time. The data are fitted by a sigmoid function (see eq 1) which provides an approximate decay time. The lifetime of the excited state is defined as the point at which half of the trajectories have decayed to the ground state. It is marked in the plots with a vertical line. The parameter K denotes the fraction of trajectories that decay until the end of the simulation.

$$f(x) = \frac{K}{1 + e^{-B(x-M)}} \qquad (1)$$

The deactivation of the α isomer may be realized through two different phototransformations — (i) the ESIPT process followed by CC bond twist or (ii) the photoisomerization around the CN bond (direct cis−trans transformation). This deactivation proceeds at an average time scale of ca. 150 fs which makes it slower by around 50 fs in comparison with the excited-state decay of the γ form (see Figure 3). Within the total simulation time of 1 ps, the internal conversion to the ground state is very efficient for both SMA forms—less than 6% (9%) of the trajectories are left in the excited state for the α (γ)
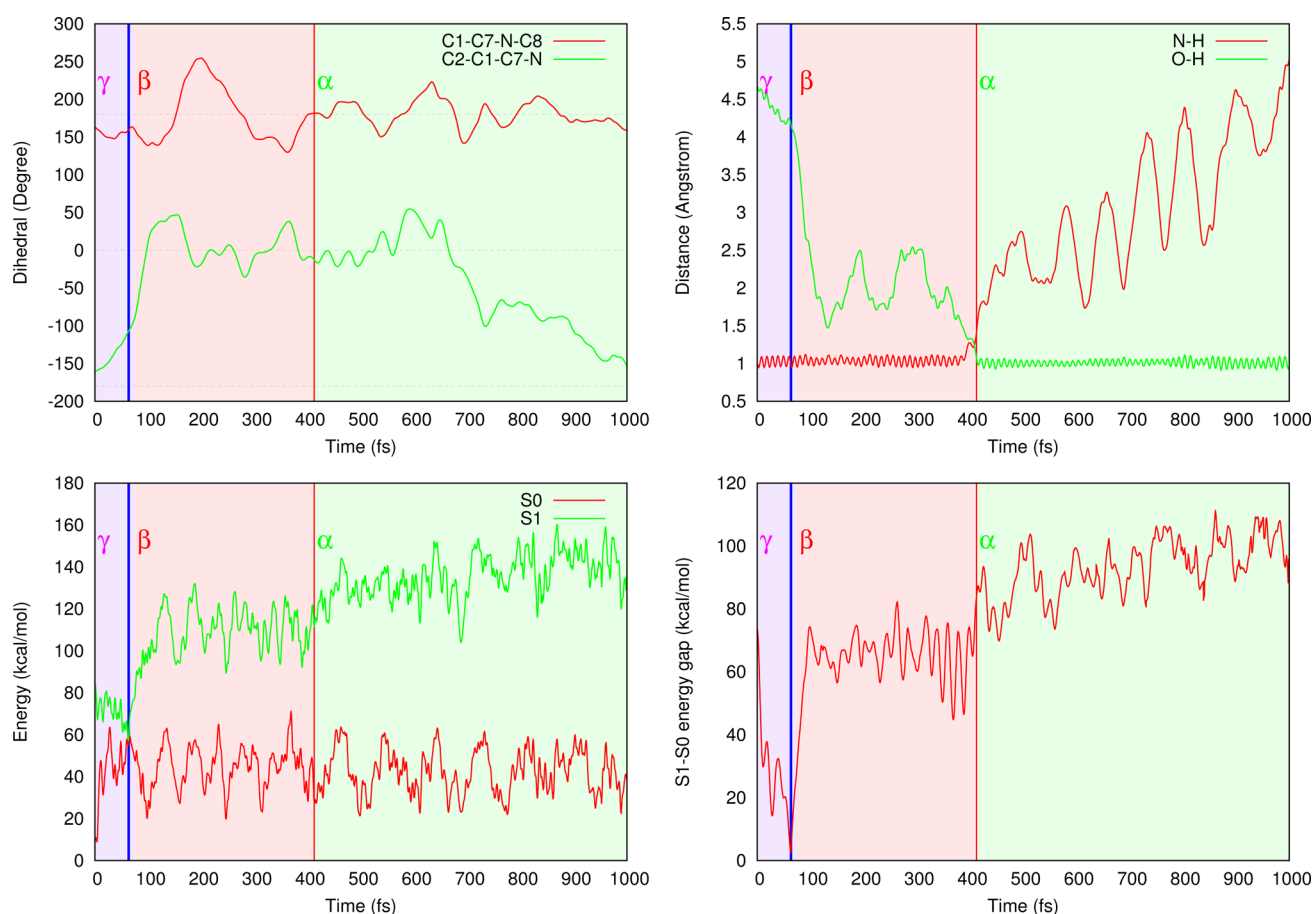
Figure 5. Different properties vs simulation time of a typical trajectory for the γ isomer. Top left: dihedrals, horizontal dashed lines mark multiples of 180°; top right: distances; bottom left: state energies; bottom right: energy difference.

photodynamics, respectively. The slightly higher number of such trajectories in the γ case may be attributed to the very flat shape of the S_1 potential energy surface (PES) in the Franck–Condon region and the lack of excess kinetic energy from ESIPT (compared with the α case).

Typical trajectories. Figure 4 and Figure 5 show the time evolution of key parameters characterizing the photodynamical trajectories of the α and γ isomers, respectively. The plots for the two sample runs include: the dihedral angle of CC and CN rotations, the OH and NH distances, the S_0 and S_1 energies relative to the global ground-state minimum of the α isomer, and the energy gap between these two states. Blue vertical lines mark the hopping events between the two energy surfaces, while the red lines indicate an intramolecular proton transfer. To facilitate the analysis of the graphs, the geometrical structures present at each stage of the dynamics are indicated by a corresponding label (i.e., α, β, γ, or δ).

Figure 4 shows a trajectory starting from the α isomer. After photoexcitation occurs an ultrafast proton transfer to the N atom (finished within 30 fs) accompanied by a clear reduction of the S_1/S_0 energy gap. A subsequent rotational motion takes the system toward the CI1 conical intersection, where it hops to the ground state at a simulation time of ca. 150 fs. This is followed by torsional oscillations around the CN bond (for ca. 700 fs); CC rotation is not feasible in the ground state, because during $S_1 \rightarrow S_0$ deactivation the π^* orbital localized at the CC bond becomes unoccupied and thus the energy barrier for CC rotation rises significantly. The ground-state proton transfer

from the nitrogen back to the oxygen atom then occurs at ca. 850 fs, regenerating the α isomer and restoring the interstate energy gap to its initial value. At this point, further CN rotation is also suppressed.

The trajectory starting from the γ isomer in Figure 5 shows a faster, single-step deactivation involving only CC bond rotation (there is no need for ESIPT to open the route toward the CI). The system hops to the ground state at ca. 70 fs and thereafter exhibits a similar behavior as on the previously discussed α trajectory. A difference between the two α and γ simulations can be seen in the OH and NH stretching amplitudes, which should be associated with the ease of proton back transfer in the ground state. After roaming on the S_0 PES in the vicinity of the β isomer for ca. 350 fs, the proton is transferred from the N back to the O atom, and the system ends up in the α form. These transformations are again accompanied by characteristic energy gap changes.

Structure population analysis. In line with a previously proposed scheme,[29] we have analyzed the SMA isomers observed during the dynamics simulations in terms of photochemical classes. Depending on the values of the three key internal degrees of freedom (CN dihedral, CC dihedral, and OH distance) we assign the starting, hopping, and final structures from each trajectory to the α, β, γ, or δ sets (for precise class definitions see the Supporting Information). Within one particular photochemical class all SMA conformers are interconvertible by rotations around single bonds that usually require only little energy. All class members have similar
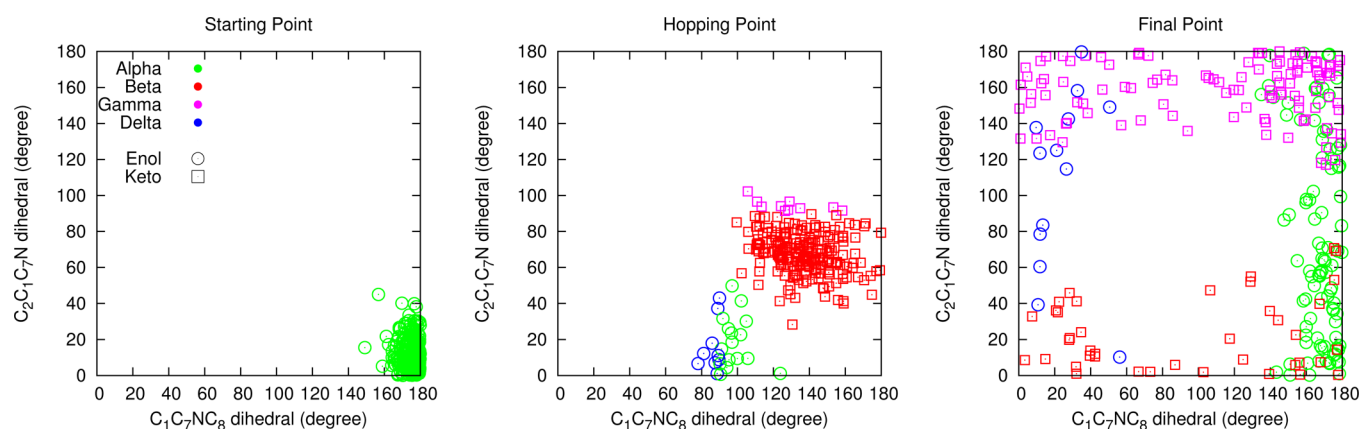
Figure 6. Dihedral angle distribution of key structures in the trajectories starting from the α isomer. Color code for assignment to isomers: green − α; red − β; violet − γ; blue − δ.
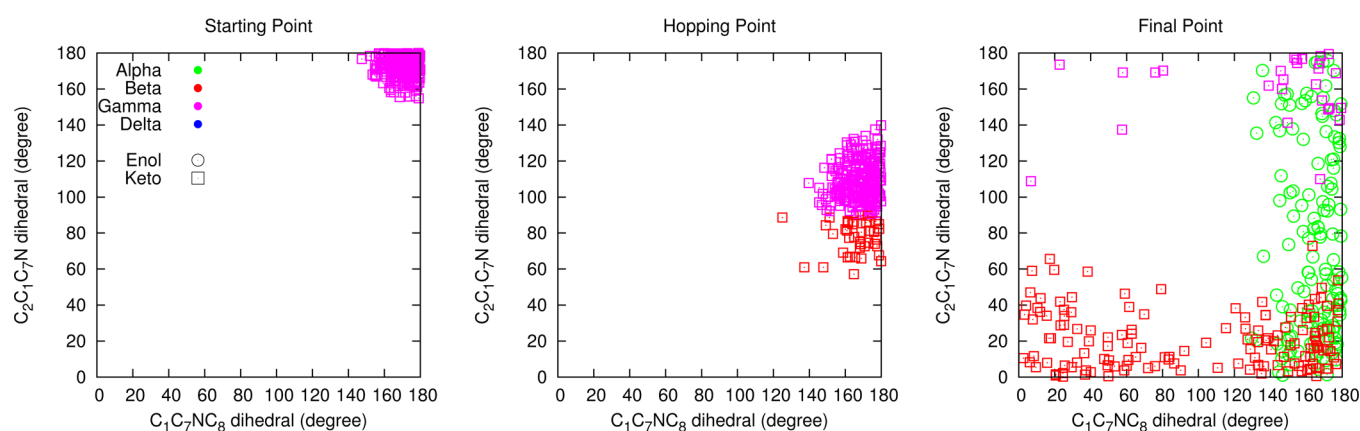

Figure 7. Dihedral angle distribution of key structures in the trajectories starting from the γ isomer. Color code for assignment to isomers: green − α; red − β; violet − γ; blue − δ.

UV absorption spectra which are, however, distinct from those of different-class representatives.

Figure 6 shows results of such a structure population analysis for the α photodynamics. At the starting point, the two key dihedral angles do not differ much from the optimum values of 0 and 180 of the initial α isomer (left panel). By contrast, the hopping points (middle panel) have twisted structures, with at least one of the two key dihedral angles differing strongly from 0 and 180°. These hopping points are concentrated in two areas: CC ≈ 90° and CN ∈ [120° −160°] and CN ≈ 90° and CC ∈ [0° − 30°]. This reflects the competition between two internal conversion pathways proceeding through the CI1 and CI2 conical intersections. The first one, involving ESIPT followed by CC bond rotation, happens much more frequently than the second one, involving CN bond photoisomerization (ca. 9:1 probability ratio). This is plausible because the path from the Franck−Condon point to CI1 is essentially barrierless and initiated by the ultrafast ESIPT process, while at the same time there is a small barrier on the route to the alternative CI2 conical intersection. In the right panel with the final structures (final points of the simulation) one finds all possible isomers in an α:β:γ:δ photoproduct distribution of ca. 7:3:9:1. Evidently, the switching forms − α and γ − are strongly preferred over the other two structures. The small amount of the δ form represents the photoproducts of the alternative deactivation mechanism via CI2. On a somewhat longer time scale, the initially produced β isomers are expected to undergo a nearly barrierless ground-state proton back transfer transforming them into the α photochemical class. The collected data also allow an estimate of the splitting ratio at both conical intersections. Comparing the overall number of final structures classified as α and β that arise from hopping around CI1 with the number of final γ isomers, one gets a 1:1 ratio. An analogous analysis for the CI2 conical intersection (involving the δ and α structures coming from the deactivation at CI2) also gives a 1:1 ratio.

The corresponding results for the γ isomer are shown in Figure 7. Again, the trajectories start in the vicinity of the initial minimum (left panel). All the hopping points lie close to the CI1 conical intersection (middle panel). They are reached from the Franck−Condon region of the γ isomer by CC bond rotation (note that CI2 cannot be accessed from the γ structure). At the end of the simulation (right panel) most of the trajectories end up as α or β isomers, with a photoproduct distribution α:β:γ:δ of ca. 4:5:1:0. Thus, the overall splitting ratio estimated for CI1 equals 9:1 for the γ photodynamics.

The product distribution in the two photodynamics simulations gives valuable information about the expected photoswitching efficiency — the extent of the initial-to-final transformation at the end of the simulation may be considered as one of its possible measures. Comparison of the α:β:γ:δ ratio for the onward (α photodynamics) and backward (γ photodynamics) switching shows better performance of the latter. The initial-to-final conversion (counting the β population as future α class) amounts to 50% for the $\alpha \rightarrow \gamma$ and to 90% for
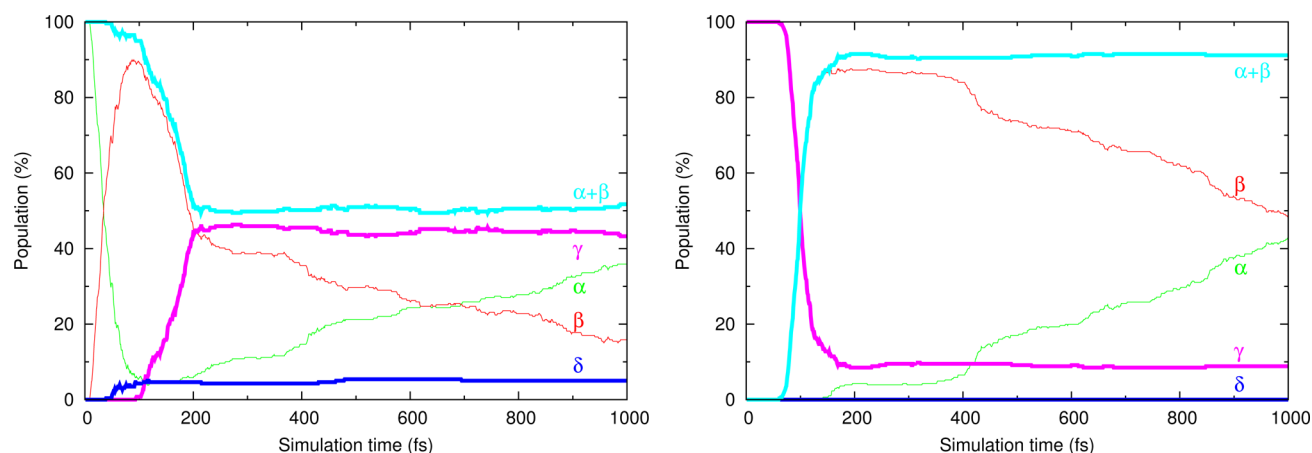
Figure 8. Abundance of the different product isomers plotted against simulation time. Color code for the isomers: green $- \alpha$; red $- \beta$; cyan $- \alpha + \beta$; violet $- \gamma$; blue $- \delta$.

the $\gamma \rightarrow \alpha$ phototransformation. These percentages almost perfectly reflect the splitting ratio at CI1 — the conical intersection responsible for the dominant internal conversion mechanism in SMA. Therefore, it is worthwhile to focus attention on the structural bifurcation at CI1. The splitting ratio may be explained in terms of the interplay between the effects of *momentum conservation* and *coupling to the local density of states*. The first factor, understood as favorable continuation of the rotational motion driving the system to a conical intersection, always supports direct passing through the CI and, thus, the photoswitching. The second one, a purely quantum effect, enters the dynamics through vibrational mode relaxation that occurs after the hop to the ground state. This vibrational cooling is more efficient for the more pronounced (deeper and/or wider) of the minima adjacent to the splitting CI point, which in our case is the α isomer. One should notice that in the α photodynamics these two effects act against each other leading to a rather even splitting distribution, while in the γ case they act in the same direction and thus favor formation of the α isomer.

Figure 8 shows the time evolution of the photochemical class populations for both photodynamics: $\alpha -$ left panel and $\gamma -$ right panel. After excitation of the α form, one observes an ultrafast α to β transformation (ESIPT) occurring mainly in the first 30 fs of the simulation; this is in very good agreement with previous theoretical results[16] and with experimental findings for similar systems.[62] Slightly later, ca. 50 fs after the excitation, the population of the δ form starts to grow which, after rising to a 5% value, stays constant until the simulation ends. This confirms, as expected, that in the S_1 state an intramolecular ballistic transfer of a light proton occurs faster than a rotation around the CN bond. Consequently, the internal conversion through CI1 plays a predominant role in SMA photodynamics. Further analysis of the left panel of Figure 8 (100 fs < t < 200 fs) shows that the β population, after reaching its maximum arising from the ESIPT process, decreases rapidly. At the same time (starting ca. 70 fs after the PT) the amount of γ isomer starts to grow with a similar rate. This reflects the internal conversion process with a bifurcation between the β and γ forms and is consistent with the previously estimated S_1 excited-state lifetime. After 200 fs the γ population stabilizes at its final value, and one observes an almost linear decrease (increase) in the population of the β (α) isomer, which continues until the end of the 1 ps simulation. Assuming this

trend to continue, the full switching process would be finished around 1.6 ps after the initial photoexcitation of the α isomer, which is again in agreement with experimental observations for analogous Schiff base systems.[62]

From the right panel of Figure 8 one may learn about the time characteristics of the back-switching process starting with an excitation of the γ form. At the very beginning the system stays close to the initial structure and then, again after ca. 70 fs, the γ to β transformation starts. This happens through internal conversion at CI1 with bifurcation between these two forms, similarly as in the previously discussed α photodynamics. Population of the β isomer initializes the subsequent β to α transformation, which again proceeds almost linearly with time. Concomitantly, the γ population reached after the S_1 to S_0 deactivation remains constant, and no traces of the δ form are observed. In analogy to the analysis for the α case, the overall γ switching time scale may be estimated as ca. 2.0 ps.

■ CONCLUSION

In this paper we investigated the full photoswitching cycle of an isolated SMA molecule by means of the semiempirical on-the-fly photodynamics simulations. For the two isomers that play a crucial role in the switching (α and γ), we find a very efficient internal conversion (~90% nonradiative decay of the excited state) that indicates excellent photostability and promising switching efficiency of SMA. The computed time scales characterizing the crucial phototransformations of this model Schiff base system are all in the ultrafast regime (~1 ps and subpicosecond). The simulations predict that the switching process is reversible in SMA and that the competing photoisomerization around the CN bond plays only a minor role in the photochemistry of this system. The detailed analysis of structural time evolution provides direct insight into the internal conversion and switching mechanisms. The strong dependence of the splitting ratio at the CI1 conical intersection on the photoswitching direction probably originates from the ground-state PES topology of the α and γ switching forms.

The ESIPT-based photoswitching mechanism in SMA involves pronounced reorganization of the electron density accompanied by only minor changes in its geometrical structure. This should allow for switching selectivity due to the strong photochromism and should also ensure structural stability, which are both important factors in the design of molecular electronics devices. In summary, we believe that

aromatic Schiff bases may have advantages over many previously proposed molecular photoswitching systems because of their ultrafast photochemistry, high photostability, and good excitation selectivity, and that they may thus be considered as promising candidates for future photodriven molecular electronics materials.

■ ASSOCIATED CONTENT

Ⓢ Supporting Information

Active space for OM2/MRCI calculations, ab initio relative energies, definition of SMA photochemical classes, and optimized Cartesian coordinates. This material is available free of charge via the Internet at http://pubs.acs.org.

■ AUTHOR INFORMATION

Corresponding Author
*E-mail: thiel@kofo.mpg.de.

Notes
The authors declare no competing financial interest.

■ ACKNOWLEDGMENTS

■ REFERENCES

(1) Yokoyama, Y. Fulgides for Memories and Switches. *Chem. Rev.* **2000**, *100*, 1717−1739.

(2) Irie, M. Diarylethenes for Memories and Switches. *Chem. Rev.* **2000**, *100*, 1685−1716.

(3) Berkovic, G.; Krongauz, V.; Weiss, V. Spiropyrans and Spirooxazines for Memories and Switches. *Chem. Rev.* **2000**, *100*, 1741−1754.

(4) Tian, H.; Yang, S. Recent progresses on diarylethene based photochromic switches. *Chem. Soc. Rev.* **2004**, *33*, 85−97.

(5) Beharry, A. A.; Woolley, G. A. Azobenzene photoswitches for biomolecules. *Chem. Soc. Rev.* **2011**, *40*, 4422−4437.

(6) Feringa, B. L.; van Delden, R. A.; Koumura, N.; Geertsema, E. M. Chiroptical Molecular Switches. *Chem. Rev.* **2000**, *100*, 1789−1816.

(7) Feringa, B. L.; Browne, W. R. *Molecular Switches*; Wiley-VCH Verlag GmbH & Co. KGaA: Weinheim, 2011.

(8) Kawata, S.; Kawata, Y. Three-Dimensional Optical Data Storage Using Photochromic Materials. *Chem. Rev.* **2000**, *100*, 1777−1788.

(9) Wuttig, M.; Yamada, N. Phase-change materials for rewriteable data storage. *Nat. Mater.* **2007**, *6*, 824−832.

(10) Raymo, F. M.; Giordani, S. All-optical processing with molecular switches. *Proc. Natl. Acad. Sci. U. S. A.* **2002**, *99*, 4941−4944.

(11) Sobolewski, A. L. Reversible molecular switch driven by excited-state hydrogen transfer. *Phys. Chem. Chem. Phys.* **2008**, *10*, 1243−1247.

(12) Łapiński, L.; Nowak, M. J.; Nowacki, J.; Rode, M. F.; Sobolewski, A. L. A Bistable Molecular Switch Driven by Photoinduced Hydrogen-Atom Transfer. *ChemPhysChem* **2009**, *10*, 2290−2295.

(13) Hadjoudis, E.; Mavridis, I. M. Photochromism and thermochromism of Schiff bases in the solid state: structural aspects. *Chem. Soc. Rev.* **2004**, *33*, 579−588.

(14) Sobolewski, A. L.; Domcke, W.; Hättig, C. Photophysics of Organic Photostabilizers. Ab Initio Study of the Excited-State Deactivation Mechanisms of 2-(2-Hydroxyphenyl)benzotriazole. *J. Phys. Chem. A* **2006**, *110*, 6301−6306.

(15) Sobolewski, A.; Domcke, W. Computational studies of the photophysics of hydrogen-bonded molecular systems. *J. Phys. Chem. A* **2007**, *111*, 11725−11735.

(16) Ortiz-Sánchez, J. M.; Gelabert, R.; Moreno, M.; Lluch, J. M. Theoretical Study on the Excited-State Intramolecular Proton Transfer in the Aromatic Schiff Base Salicylidene Methylamine: an Electronic Structure and Quantum Dynamical Approach. *J. Phys. Chem. A* **2006**, *110*, 4649−4656.

(17) Ortiz-Sánchez, J. M.; Gelabert, R.; Moreno, M.; Lluch, J. M. Electronic-structure and quantum dynamical study of the photochromism of the aromatic Schiff base salicylideneaniline. *J. Chem. Phys.* **2008**, *129*, 214308.

(18) Migani, A.; Blancafort, L.; Robb, M. A.; DeBellis, A. D. An Extended Conical Intersection Seam Associated with a Manifold of Decay Paths: Excited-State Intramolecular Proton Transfer in o-Hydroxybenzaldehyde. *J. Am. Chem. Soc.* **2008**, *130*, 6932−6933.

(19) Szymański, W.; Beierle, J. M.; Kistemaker, H. A. V.; Velema, W. A.; Feringa, B. L. Reversible Photocontrol of Biological Systems by the Incorporation of Molecular Photoswitches. *Chem. Rev.* **2013**, *113*, 6114−6178.

(20) Otsubo, N.; Okabe, C.; Mori, H.; Sakota, K.; Amimoto, K.; Kawato, T.; Sekiya, H. Excited-state intramolecular proton transfer in photochromic jet-cooled salicylideneaniline. *J. Photochem. Photobiol., A* **2002**, *154*, 33−39.

(21) Mitra, S.; Tamai, N. Dynamics of photochromism in salicylideneaniline: A femtosecond spectroscopic study. *Phys. Chem. Chem. Phys.* **2003**, *5*, 4647−4652.

(22) Ziółek, M.; Kubicki, J.; Maciejewski, A.; Naskręcki, R.; Grabowska, A. An ultrafast excited state intramolecular proton transfer (ESPIT) and photochromism of salicylideneaniline (SA) and its "double" analogue salicylaldehyde azine (SAA). A controversial case. *Phys. Chem. Chem. Phys.* **2004**, *6*, 4682−4689.

(23) Okabe, C.; Nakabayashi, T.; Inokuchi, Y.; Nishi, N.; Sekiya, H. Ultrafast excited-state dynamics in photochromic N-salicylideneaniline studied by femtosecond time-resolved REMPI spectroscopy. *J. Chem. Phys.* **2004**, *121*, 9436−9442.

(24) Sliwa, M.; Mouton, N.; Ruckebusch, C.; Poisson, L.; Idrissi, A.; Alose, S.; Potier, L.; Dubois, J.; Poizat, O.; Buntinx, G. Investigation of ultrafast photoinduced processes for salicylidene aniline in solution and gas phase: toward a general photo-dynamical scheme. *Photochem. Photobiol. Sci.* **2010**, *9*, 661−669.

(25) Spörkel, L.; Cui, G.; Thiel, W. Photodynamics of Schiff Base Salicylideneaniline: Trajectory Surface-Hopping Simulations. *J. Phys. Chem. A* **2013**, *117*, 4574−4583.

(26) Zgierski, M. Z.; Grabowska, A. Theoretical approach to photochromism of aromatic Schiff bases: A minimal chromophore salicylidene methylamine. *J. Chem. Phys.* **2000**, *113*, 7845−7852.

(27) Knyazhansky, M.; Metelitsa, A.; Kletskii, M.; Millov, A.; Besugliy, S. The structural transformations and photo-induced processes in salicylidene alkylimines. *J. Mol. Struct.* **2000**, *526*, 65−79.

(28) Grabowska, A.; Kownacki, K. Structural aspects of photochromism of the internally H-bonded Schiff bases. "A minimal chromophore". *Acta Phys. Polym., A* **1995**, *88*, 1081−1088.

(29) Jankowska, J.; Rode, M. F.; Sadlej, J.; Sobolewski, A. L. Photophysics of Schiff Bases: Theoretical Study of Salicylidene Methylamine. *ChemPhysChem* **2012**, *13*, 4287−4294.

(30) Weber, W. Ph.D. Thesis, University of Zürich, 1996.

(31) Weber, W.; Thiel, W. Orthogonalization corrections for semiempirical methods. *Theor. Chem. Acc.* **2000**, *103*, 495−506.

(32) Koslowski, A.; Beck, M.; Thiel, W. Implementation of a general multireference configuration interaction procedure with analytic gradients in a semiempirical context using the graphical unitary group approach. *J. Comput. Chem.* **2003**, *24*, 714−726.

(33) Thiel, W. *MNDO99 program*, version 6.1. 2007; Max-Planck-Institut für Kohlenforschung: Mülheim, Germany, 2007.

(34) Dewar, M. J. S.; Hashmall, J. A.; Venier, C. G. Ground states of conjugated molecules. IX. Hydrocarbon radicals and radical ions. *J. Am. Chem. Soc.* **1968**, *90*, 1953−1957.

(35) Silva-Junior, M.; Thiel, W. Benchmark of Electronically Excited States for Semiempirical Methods: MNDO, AM1, PM3, OM1, OM2, OM3, INDO/S, and INDO/S2. *J. Chem. Theory Comput.* **2010**, *6*, 1546−1564.

(36) Fabiano, E.; Thiel, W. Nonradiative deexcitation dynamics of 9H-adenine: An OM2 surface hopping study. *J. Phys. Chem. A* **2008**, *112*, 6859−6863.

(37) Lan, Z.; Fabiano, E.; Thiel, W. Photoinduced Nonadiabatic Dynamics of Pyrimidine Nucleobases: On-the-Fly Surface-Hopping Study with Semiempirical Methods. *J. Phys. Chem. B* **2009**, *113*, 3548−3555.

(38) Lan, Z.; Fabiano, E.; Thiel, W. Photoinduced Nonadiabatic Dynamics of 9H-Guanine. *ChemPhysChem* **2009**, *10*, 1225−1229.

(39) Lan, Z.; Lu, Y.; Fabiano, E.; Thiel, W. QM/MM Nonadiabatic Decay Dynamics of 9H-Adenine in Aqueous Solution. *ChemPhysChem* **2011**, *12*, 1989−1998.

(40) Lu, Y.; Lan, Z.; Thiel, W. Hydrogen Bonding Regulates the Monomeric Nonradiative Decay of Adenine in DNA Strands. *Angew. Chem., Int. Ed.* **2011**, *50*, 6864−6867.

(41) Weingart, O.; Lan, Z.; Koslowski, A.; Thiel, W. Chiral Pathways and Periodic Decay in cis-Azobenzene Photodynamics. *J. Phys. Chem. Lett.* **2011**, *2*, 1506−1509.

(42) Kazaryan, A.; Lan, Z.; Schäfer, L.; Thiel, W.; Filatov, M. Surface Hopping Excited-State Dynamics Study of the Photoisomerization of a Light-Driven Fluorene Molecular Rotary Motor. *J. Chem. Theory Comput.* **2011**, *7*, 2189−2199.

(43) Lan, Z.; Lu, Y.; Weingart, O.; Thiel, W. Nonadiabatic Decay Dynamics of a Benzylidene Malononitrile. *J. Phys. Chem. A* **2012**, *116*, 1510−1518.

(44) Lu, Y.; Lan, Z.; Thiel, W. Monomeric adenine decay dynamics influenced by the DNA environment. *J. Comput. Chem.* **2012**, *33*, 1225−1235.

(45) Cui, G.; Lan, Z.; Thiel, W. Intramolecular hydrogen bonding plays a crucial role in the photophysics and photochemistry of the GFP chromophore. *J. Am. Chem. Soc.* **2012**, *134*, 1662−1672.

(46) Cui, G.; Thiel, W. Nonadiabatic dynamics of a truncated indigo model. *Phys. Chem. Chem. Phys.* **2012**, *14*, 12378−12384.

(47) Cui, G.; Thiel, W. Photoinduced Ultrafast Wolff Rearrangement: A Non-Adiabatic Dynamics Perspective. *Angew. Chem., Int. Ed.* **2013**, *52*, 433−436.

(48) Spörkel, L.; Cui, G.; Koslowski, A.; Thiel, W. Nonequilibrium H/D Isotope Effects from Trajectory-Based Nonadiabatic Dynamics. *J. Phys. Chem. A* **2014**, *118*, 152−157.

(49) Wigner, E. On the quantum correction for thermodynamic equilibrium. *Phys. Rev.* **1932**, *40*, 749−759.

(50) Barbatti, M.; Granucci, G.; Persico, M.; Ruckenbauer, M.; Vazdar, M.; Eckert-Maksić, M.; Lischka, H. The on-the-fly surface-hopping program system Newton-X: Application to ab initio simulation of the nonadiabatic photodynamics of benchmark systems. *J. Photochem. Photobiol., A* **2007**, *190*, 228−240.

(51) Martyna, G.; Klein, M.; Tuckerman, M. Nose-Hoover chains: The canonical ensemble via continuous dynamics. *J. Chem. Phys.* **1992**, *97*, 2635−2643.

(52) Otte, N.; Scholten, M.; Thiel, W. Looking at Self-Consistent-Charge Density Functional Tight Binding from a Semiempirical Perspective. *J. Phys. Chem. A* **2007**, *111*, 5751−5755.

(53) Elstner, M.; Porezag, D.; Jungnickel, G.; Elsner, J.; Haugk, M.; Frauenheim, T.; Suhai, S.; Seifert, G. Self-consistent-charge density-functional tight-binding method for simulations of complex materials properties. *Phys. Rev. B* **1998**, *58*, 7260−7268.

(54) Cui, Q.; Elstner, M.; Kaxiras, E.; Frauenheim, T.; Karplus, M. A QM/MM Implementation of the Self-Consistent Charge Density Functional Tight Binding (SCC-DFTB) Method. *J. Phys. Chem. B* **2001**, *105*, 569−585.

(55) Tully, J. Molecular dynamics with electronic transitions. *J. Chem. Phys.* **1990**, *93*, 1061−1071.

(56) Hammes-Schiffer, S.; Tully, J. Proton transfer in solution: Molecular dynamics with quantum transitions. *J. Chem. Phys.* **1994**, *101*, 4657−4667.

(57) Fabiano, E.; Keal, T.; Thiel, W. Implementation of surface hopping molecular dynamics using semiempirical methods. *Chem. Phys.* **2008**, *349*, 334−347.

(58) Keal, T.; Wanko, M.; Thiel, W. Assessment of semiempirical methods for the photoisomerisation of a protonated Schiff base. *Theor. Chem. Acc.* **2009**, *123*, 145−156.

(59) Granucci, G.; Persico, M.; Zoccante, A. Including quantum decoherence in surface hopping. *J. Chem. Phys.* **2010**, *133*, 134111.

(60) ChemShell3.4, a Computational Chemistry Shell; see www.chemshell.org.

(61) Metz, S.; Kästner, J.; Sokol, A.; Keal, T.; Sherwood, P. ChemShell—a modular software package for QM/MM simulations. *WIREs Comput. Mol. Sci.* **2014**, *4*, 101−110.

(62) Ziółek, M.; Kubicki, J.; Maciejewski, A.; Naskręcki, R.; Grabowska, A. Excited state proton transfer and photochromism of an aromatic Schiff base. Pico-and femtosecond kinetics of the salicylidene phenylenediamine. *Chem. Phys. Lett.* **2003**, *369*, 80−89.